

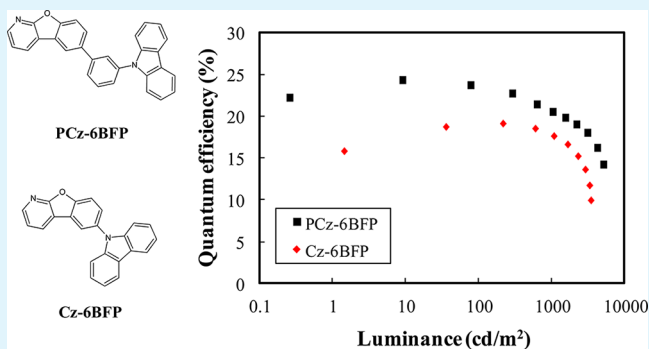
High Quantum Efficiency Blue Phosphorescent Organic Light-Emitting Diodes Using 6-Position-Modified Benzofuro[2,3-b]pyridine Derivatives

Chil Won Lee,[†] Jung-Keun Kim,[‡] Sung Hoon Joo,[‡] and Jun Yeob Lee^{*,†}

[†]Department of Polymer Science and Engineering, Dankook University 126, Jukjeon-dong, Suji-gu, Yongin-si, Gyeonggi-do 448-701, Korea

[‡]LG Display R&D Center, 1007 Deogeun-ri, Wollong-myeon, Paju-si, Gyeonggi-do, 413-811, Korea

ABSTRACT: High quantum efficiency blue phosphorescent organic light-emitting diodes were developed using 6-position modified benzofuro[2,3-b]pyridine derivatives as host materials. Two high triplet energy host materials derived from benzofuro[2,3-b]pyridine modified with carbazole or 9-phenylcarbazole were synthesized and the device performances of the host materials were investigated. A high quantum efficiency of 24.3% was achieved using the benzofuro[2,3-b]pyridine host materials due to good charge balance and energy transfer.



KEYWORDS: benzofuro[2,3-b]pyridine, bipolar host, high triplet energy, carbazole, phosphorescence

INTRODUCTION

Bipolar host materials have been generally used as the host materials for blue phosphorescent organic light-emitting diodes (PHOLEDs) because high quantum efficiency was achieved through holes and electrons balance in the emitting layer.^{1,2} High quantum efficiency above 20% has already been reported in blue PHOLEDs using the bipolar host materials.^{3–8}

In general, bipolar host materials have hole transport and electron transport moieties in the molecular structure for bipolar charge transport properties. Typically, carbazole has been used as the hole transport unit,^{3–6,8–13} whereas diphenylphosphine oxide modified aromatic unit,^{5,6,8} pyridine,^{3,9} triazine,^{10,11} imidazole,¹⁴ and cyano-substituted arylene^{15,16} have been adopted as electron transport units. The combination of the hole transport and electron transport units produced high triplet energy bipolar host materials for blue PHOLEDs and high quantum efficiency was obtained using the host materials. However, the number of electron transport moieties applicable to high triplet energy bipolar host materials is limited and further development of electron transport unit is strongly required.

Recently, we reported benzofuro[2,3-b]pyridine (BFP) as a new electron transport unit for high triplet energy bipolar host materials.¹⁷ The BFP moiety was modified with 9-phenylcarbazole at 3-position to develop the bipolar host material, 3-(3-(carbazole-9-yl)phenyl)benzofuro[2,3-b]pyridine (PCz-BFP). High quantum efficiency was reported using the PCz-BFP in solution and vacuum-processed blue PHOLEDs because of stable film morphology and bipolar charge transport properties.

In this work, we modified the BFP electron deficient core at 6-position to further improve the device performances of blue PHOLEDs. 6-Chloro[1]benzofuro[2,3-b]pyridine (6Cl-BFP) was newly synthesized as the intermediate compound for substitution of 9-phenylcarbazole or carbazole at 6-position of BFP. Two host materials, 6-(carbazole-9-yl)benzofuro[2,3-b]pyridine (Cz-6BFP) and 6-(3-(carbazole-9-yl)phenyl)benzofuro[2,3-b]pyridine (PCz-6BFP), were developed as the high triplet energy host materials for blue PHOLEDs. It was demonstrated that high quantum efficiency of 24.3% was achieved using the PCz-6BFP host material.

EXPERIMENTAL SECTION

General Information. 2-Amino-3-bromopyridine and other important reagents were purchased from Aldrich and TCI Chem. All reactions were carried out under a N₂ atmosphere. 3-(Carbazol-9-yl)phenylboronic acid (3-CzPBA) was prepared according to literature.¹⁸

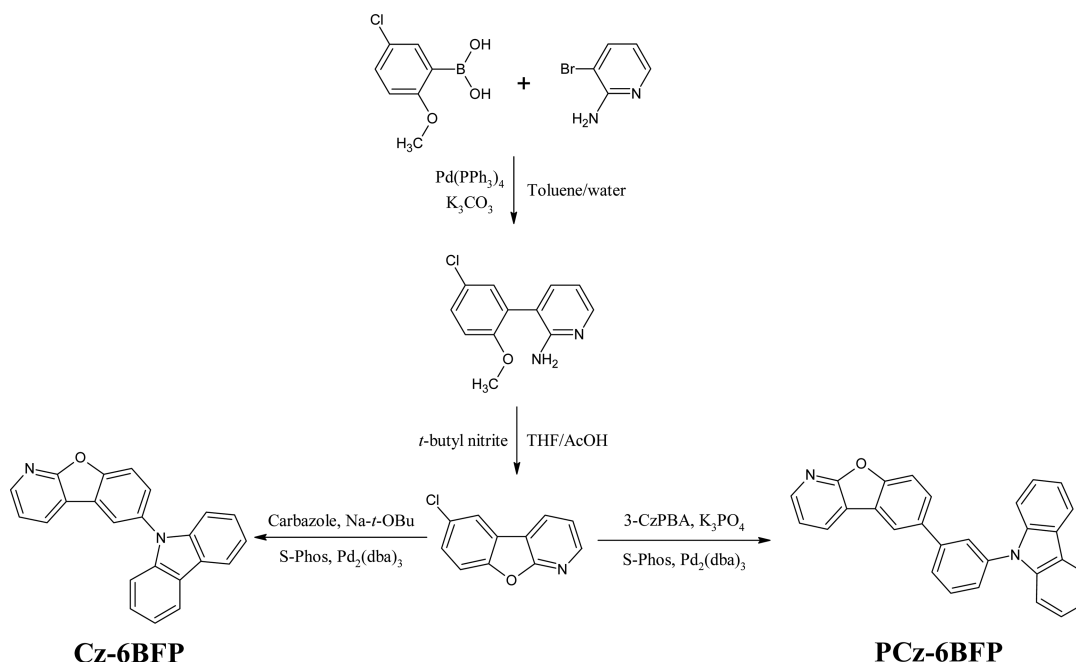
The ¹H and ¹³C nuclear magnetic resonance (NMR) were recorded on Avance 500 (Bruker). The attenuated total reflection (ATR) Fourier transform-infrared (FT-IR) spectra for all the samples were obtained using a Nicolet 380 FT-IR spectrometer. The FT-IR spectra were gathered with zinc selenide anvil ATR accessory using 32 scans at a resolution of 16 cm⁻¹. The mass spectra were recorded using a JEOL, JMS-600W spectrometer in fast atom bombardment mode. Elemental analysis of the materials was carried out using Flash2000 (ThermoFisher). The differential scanning calorimetric (DSC)

Received: December 27, 2012

Accepted: February 21, 2013

Published: February 21, 2013

Scheme 1. Synthetic Scheme of PCz-6BFP and Cz-6BFP



measurements were performed on a Mettler DSC822e under nitrogen at a heating rate of 10 °C/min. The photoluminescence (PL) spectra were recorded on a fluorescence spectrophotometer (HITACHI, F-7000) and the ultraviolet–visible (UV–vis) spectra were obtained by means of a UV–vis spectrophotometer (Shimadzu, UV-2501PC). Sample was dissolved in tetrahydrofuran at a concentration of 1.0×10^{-4} M for UV–vis and PL measurements. Triplet energy analysis was carried out using the same solution at 77 K. The highest occupied molecular orbital (HOMO) of compounds was measured with a cyclic voltammetry.

Synthesis. 3-(5-Chloro-2-methoxyphenyl)pyridin-2-amine. A solution of 2-amino-3-bromopyridine (9.0 g, 51.0 mmol), 5-chloro-2-methoxyphenyl boronic acid (10.0 g, 51.0 mmol), potassium carbonate (21.2 g, 153 mmol), 300 mL of toluene and 150 mL of distilled water was stirred and bubbled with N₂ gas for 30 min. Tetrakis(triphenylphosphine)palladium(0) (1.1 g, 1.0 mmol) was added to the solution and the resulting solution was refluxed for 24 h. The solution was cooled down to room temperature and was extracted with ethyl acetate and distilled water. The organic layer was dried over anhydrous magnesium sulfate and evaporated in vacuo to give the crude product, which was purified by column chromatography on silica gel with *n*-hexane/ethyl acetate gradient mixture as eluent, providing 8.2 g of 3-(5-chloro-2-methoxyphenyl)pyridin-2-amine.

3-(5-Chloro-2-methoxyphenyl)pyridin-2-amine. Yield: 67%. MS (FAB) m/z 235 [(M+H)⁺]. ¹H NMR (500 MHz, CDCl₃): δ 3.80 (s, 3H), 4.47 (s, 2H), 6.73 (t, 1H, $J = 4.0$ Hz), 6.92 (d, 1H, $J = 4.5$ Hz), 7.23 (s, 1H), 7.32 (m, 2H), 8.10 (d, 1H, $J = 3.5$ Hz).

6-Chlorobenzofuro[2,3-*b*]pyridine (6Cl-BFP). 3-(5-Chloro-2-methoxyphenyl)pyridin-2-amine (8.0 g, 34.1 mmol) in tetrahydrofuran (50 mL) and glacial acetic acid (80 mL) were stirred at –10 °C and *tert*-butyl nitrite (10.5 g, 102 mmol) was added via syringe over a period of 20 min. After stirring for 1 h. at –10 °C, the solution was stirred at 0 °C over a period of 12 h. The reaction mixture was warmed to room temperature and diluted with 150 mL of water. Precipitated material was filtered and dried, providing 4.1 g of pure 6Cl-BFP.

6Cl-BFP. Yield 59%. MS (FAB) m/z 204 [(M+H)⁺]. ¹H NMR (500 MHz, CDCl₃): δ 7.36 (t, 1H, $J = 4.2$ Hz), 7.49 (d, 1H, $J = 5.5$ Hz), 7.58 (d, 1H, $J = 4.5$ Hz), 7.93 (s, 1H), 8.25 (d, 1H, $J = 4.5$ Hz), 8.49 (d, 1H, $J = 3.2$ Hz).

6-(Carbazole-9-yl)benzofuro[2,3-*b*]pyridine (Cz-6BFP). A mixture of 6Cl-BFP (1.5 g, 7.37 mmol), carbazole (1.48 g, 8.84 mmol), sodium *tert*-butoxide (1.7 g, 17.7 mmol), 2-dicyclohexylphosphino-2',6'-

dimethoxybiphenyl (0.36 g, 0.884 mmol), and tris-(dibenzylideneacetone)dipalladium (0.20 g, 0.221 mmol) in xylene (75 mL) was refluxed for 36 h. The reaction mixture was then cooled to room temperature, and extracted with ethyl acetate/water. The organic layer was dried over anhydride magnesium sulfate, filtered, and evaporated to yield a dark brown solid. The crude material was purified by column chromatography on silica gel using dichloromethane/*n*-hexane as an eluent. Additional purification by sublimation (200 °C. at 1×10^{-5} mm Hg) resulted in 1.3 g of pure compound.

Yield 53%. mp 134 °C. FT-IR (ATR) 3054, 1590, 1417, 1451, 1392, 1335, 1230, 1186, 1116, 869, 749, 699 cm⁻¹. ¹H NMR (500 MHz, CDCl₃): δ 7.29 (t, 2H, $J = 5.2$ Hz), 7.35 (m, 3H), 7.40 (t, 2H, $J = 5.3$ Hz), 7.67 (d, 1H, $J = 5.5$ Hz), 7.83 (d, 1H, $J = 4.3$ Hz), 8.08 (s, 1H, $J = 2.5$ Hz), 8.16 (d, 2H, $J = 4.0$ Hz), 8.22 (d, 1H, $J = 4.5$ Hz), 8.50 (d, 1H, $J = 3.2$ Hz). ¹³C NMR (125 MHz, CDCl₃): δ 109.5, 113.5, 116.5, 119.4, 120.0, 120.4, 123.3, 123.9, 126.0, 127.8, 130.1, 133.3, 141.4, 147.2, 153.3, 163.8. MS (FAB) m/z 335 [(M+H)⁺]. Anal. Calcd for C₂₃H₁₄N₂O: C, 82.62%; H, 4.22%; N, 8.38%. Found: C, 82.66%; H, 4.23%; N, 8.33%.

6-(3-(Carbazole-9-yl)phenyl)benzofuro[2,3-*b*]pyridine (PCz-6BFP). A mixture of 6Cl-BFP (1.5 g, 7.37 mmol), 3-CzPBA (2.54 g, 8.84 mmol), potassium phosphate tribasic (4.69 g, 22.1 mmol), 2-dicyclohexylphosphino-2',6'-dimethoxybiphenyl (0.45 g, 1.11 mmol), tris(dibenzylideneacetone)dipalladium (0.20 g, 0.22 mmol) in toluene (150 mL) and distilled water (15 mL) was refluxed for 36 h. The solution was cooled to room temperature, diluted with 50 mL of water and extracted with ethyl acetate. The organic extracts were dried over anhydride magnesium sulfate, filtered, and evaporated to yield a brown solid. The crude material was purified by column chromatography on silica gel using dichloromethane/*n*-hexane as an eluent. Additional purification by sublimation (230 °C. at 1×10^{-5} mm Hg) resulted in 1.6 g of pure white compound.

Yield 53%. mp 159 °C. FT-IR (ATR) 3059, 1694, 1593, 1451, 1390, 1313, 1228, 1190, 1119, 1019, 927, 858, 792, 748, 725, 700 cm⁻¹. ¹H NMR (500 MHz, CDCl₃): δ 7.30 (m, 3H), 7.42 (t, 2H, $J = 5.2$ Hz), 7.48 (d, 2H, $J = 4.0$ Hz), 7.57 (d, 1H, $J = 3.8$ Hz), 7.69 (t, 2H, $J = 5.3$ Hz), 7.73 (s, 1H), 7.76 (t, 1H, $J = 6.2$ Hz), 7.84 (s, 1H), 8.16 (m, 3H), 8.24 (d, 1H, $J = 4.5$ Hz), 8.45 (d, 1H, $J = 3.0$ Hz). ¹³C NMR (125 MHz, CDCl₃): δ 109.7, 112.5, 116.8, 119.3, 119.8, 120.0, 120.4, 123.1, 123.5, 125.9, 125.9, 126.0, 126.3, 127.7, 129.7, 130.4, 135.9, 138.4, 140.9, 142.8, 146.7, 154.3, 163.6. MS (FAB) m/z 411 [(M+H)⁺]. Anal.

Calcd for $C_{29}H_{18}N_2O$: C, 84.86%; H, 4.42%; N, 6.82%. Found: C, 84.75%; H, 4.40%; N, 6.72%.

Device Fabrication and Measurements. The device structure of PHOLEDs was indium tin oxide (ITO, 50 nm)/poly(3,4-ethylenedioxythiophene);poly(styrenesulfonate) (PEDOT:PSS, 60 nm)/4,4'-cyclohexylidenebis[N,N-bis(4-methylphenyl)aniline] (TAPC, 30 nm)/PCz-6BFP or Cz-6BFP: iridium(III) bis[(4,6-difluorophenyl)pyridinato-N,C²]picolinate (FIrpic) (25 nm, 3%)/diphenylphosphine oxide-4-(triphenylsilyl)phenyl (TSPO1, 30 nm)/LiF (1 nm)/Al (200 nm). Hole only device had the device structure of ITO (50 nm)/PEDOT:PSS (60 nm)/TAPC (30 nm)/PCz-6BFP or Cz-6BFP (25 nm)/Al, and the device structure of electron only device was ITO (50 nm)/Ca (10 nm)/PCz-6BFP or Cz-6BFP (25 nm)/TSPO1 (30 nm)/LiF (1 nm)/Al (200 nm). The PEDOT:PSS layer was spin coated on UV/O₃ treated ITO surface at a spin speed of 2,000 rpm followed by baking at 150 °C for 10 min on hot plate. Other organic materials except FIrpic (0.003 nm/s) were deposited by vacuum thermal evaporation at a deposition rate of 0.1 nm/s. All devices were encapsulated with a glass lid and CaO getter after Al deposition. The device performances were measured with Keithley 2400 source measurement unit and CS1000 spectroradiometer under ambient condition.

RESULTS AND DISCUSSION

The PCz-6BFP and Cz-6BFP were designed to substitute 9-phenylcarbazole or carbazole at 6-position of the BFP electron deficient core. Compared with the PCz-BFP host with the 9-phenylcarbazole substituted to the pyridine unit of the BFP core,¹⁷ the PCz-6BFP host had the 9-phenylcarbazole attached to the benzene unit of the BFP core. The different location of the 9-phenylcarbazole may affect the charge transport properties of the host materials. The Cz-6BFP host was also synthesized as a bipolar host material derived from 6Cl-BFP.

The PCz-6BFP and Cz-6BFP were synthesized from 6Cl-BFP which was prepared by ring closing reaction of 3-(5-chloro-2-methoxyphenyl)pyridin-2-amine. The 3-(5-chloro-2-methoxyphenyl)pyridin-2-amine intermediate was synthesized by Suzuki coupling reaction of 2-amino-3-bromopyridine with 5-chloro-2-methoxyphenyl boronic acid. The 6Cl-BFP intermediate was reacted with 3-(9H-carbazol-9-yl)phenylboronic acid and 9H-carbazole to yield PCz-6BFP and Cz-6BFP, respectively. Synthetic yield of PCz-6BFP and Cz-6BFP was 53% after vacuum sublimation. The two host materials were purified by column chromatography followed by vacuum sublimation. Synthetic scheme of host materials is shown in Scheme 1.

Photophysical properties of PCz-6BFP and Cz-6BFP were analyzed using ultraviolet–visible (UV–vis) and photoluminescence (PL) spectrometer. Figure 1 shows UV–vis and PL spectra of PCz-6BFP and Cz-6BFP. Two host materials exhibited similar UV–vis absorption spectra with $n-\pi^*$ transition of carbazole between 310 and 350 nm, and $\pi-\pi^*$ transition of carbazole modified BFP at 297 and 243 nm. Bandgaps of PCz-6BFP and Cz-6BFP were calculated from the absorption edge of the UV–vis spectra and were 3.58 and 3.53 eV, respectively. PL emission of PCz-6BFP and Cz-6BFP was observed at 391 and 399 nm, respectively. Low-temperature PL analysis was also carried out to measure the triplet energy of the host materials. The triplet energies of PCz-6BFP and Cz-6BFP calculated from the first phosphorescent emission peak were 2.91 and 2.90 eV, respectively. Although the PCz-6BFP host had phenyl linkage between carbazole and BFP, the phenyl linkage did not affect the triplet energy because the conjugation of BFP was not extended. Compared with the PCz-BFP host reported earlier, there was little difference of photophysical

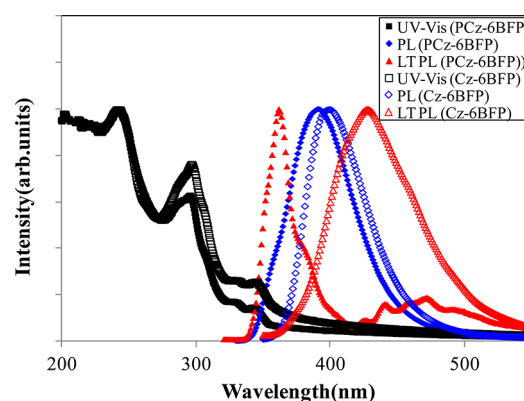


Figure 1. UV–vis absorption (room temperature, in THF), PL (room temperature, excitation with 300 nm, in THF), and low-temperature PL (77K, excitation with 300 nm, in THF) spectra of PCz-6BFP and Cz-6BFP.

properties. This indicates that the substitution position of 9-phenylcarbazole to BFP does not affect the photophysical properties of BFP derivatives.

Molecular simulation of PCz-6BFP and Cz-6BFP was performed to study the highest occupied molecular orbital (HOMO) and the lowest unoccupied molecular orbital (LUMO) distribution of the host materials. The HOMO and LUMO distribution of PCz-6BFP and Cz-6BFP is shown in Figure 2. The HOMO of PCz-6BFP was localized on the

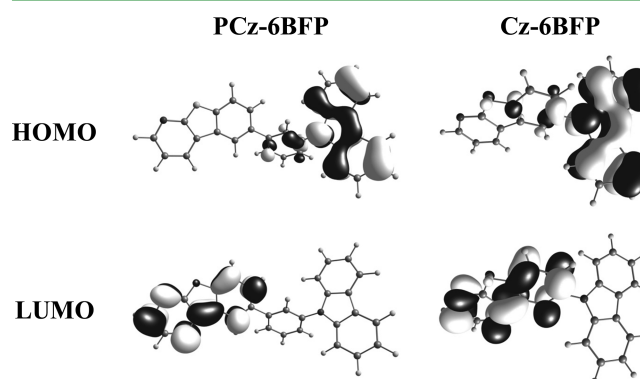


Figure 2. HOMO and LUMO distribution of PCz-6BFP and Cz-6BFP.

carbazole, whereas the LUMO was dispersed over electron deficient BFP unit. Similar HOMO and LUMO distribution was observed in Cz-6BFP even though the HOMO was slightly extended to the BFP unit. As the hole transport carbazole and electron transport BFP units were introduced in the molecular structure, the HOMO and LUMO were separated. The HOMO level of two host materials was measured by cyclic voltammetry. The HOMO/LUMOs of PCz-6BFP and Cz-6BFP were -6.10 eV/ -2.52 eV and -6.09 eV/ -2.56 eV, respectively. The LUMO was calculated from the HOMO and bandgap from UV–vis absorption edge of the UV–vis spectra. Energy levels of the host materials are summarized in Table 1.

Hole only and electron only devices of PCz-6BFP and Cz-6BFP were fabricated to compare hole and electron transport properties of the host materials. Current density–voltage curves of hole and electron only devices are shown in Figure 3. Both hole and electron current densities of Cz-6BFP were higher than those of PCz-6BFP because of small molecular size

Table 1. Energy Levels of Host Materials

material	HOMO (eV)	LUMO (eV)	bandgap (eV)	triplet energy (eV)
PCz-6BFP	-6.10	-2.52	3.58	2.91
Cz-6BFP	-6.09	-2.56	3.53	2.90

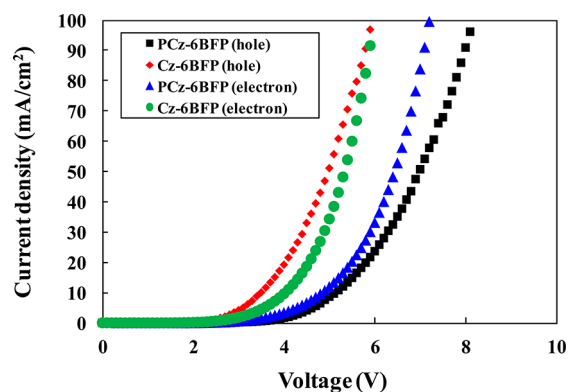


Figure 3. Current density–voltage curves of hole only and electron only devices of PCz-6BFP and Cz-6BFP.

of Cz-6BFP. Comparing the hole and electron current densities, PCz-6BFP showed higher electron current density than hole current density, while Cz-6BFP exhibited similar hole and electron current densities. The wide dispersion of the HOMO in Cz-6BFP may improve the hole transport properties because of a large integral for hole transport and may be responsible for the relatively similar hole and electron current densities. Compared with the PCz-BFP host which showed similar hole and electron current densities,¹⁷ the PCz-6BFP host possessed high electron current density. This indicates that the substitution of 9-phenylcarbazole at 6-position of BFP is effective to improve the electron transport properties of the host materials. Although there was little difference of energy levels and molecular orbital distribution, the location of the electron deficient pyridine unit affected the electron transport properties possibly because of less steric hindrance of electron accepting pyridine unit.

As PCz-6BFP and Cz-6BFP were suitable as the host materials for blue PHOLEDs because of high triplet energy and bipolar charge transport properties, blue PHOLEDs were fabricated using the host materials. Device structure of blue PHOLEDs was ITO (50 nm)/PEDOT:PSS (60 nm)/TAPC (30 nm)/PCz-6BFP or Cz-6BFP:FIrpic (25 nm, 3%)/TSPO1 (30 nm)/LiF (1 nm)/Al (200 nm). Current density–voltage–luminance curves of the blue PHOLEDs are shown in Figure 4. The current density was high in the Cz-6BFP device because of high hole and electron current densities as shown in Figure 3. However, the luminance of the Cz-6BFP was similar to that of the PCz-6BFP device, implying low recombination efficiency of the Cz-6BFP device.

Quantum efficiency–luminance curves of the PCz-6BFP and Cz-6BFP blue PHOLEDs are shown in Figure 5. The PCz-6BFP device showed much higher quantum efficiency than the Cz-6BFP device over all luminance range. The maximum quantum efficiency of the PCz-6BFP device was 24.3% and the quantum efficiency at 1,000 cd/m² was 20.6% compared with the maximum quantum efficiency of 19.1% and the quantum efficiency at 1,000 cd/m² of 17.7% of the Cz-6BFP device. The difference of quantum efficiency between the two host materials can be explained by the hole and electron current density of the

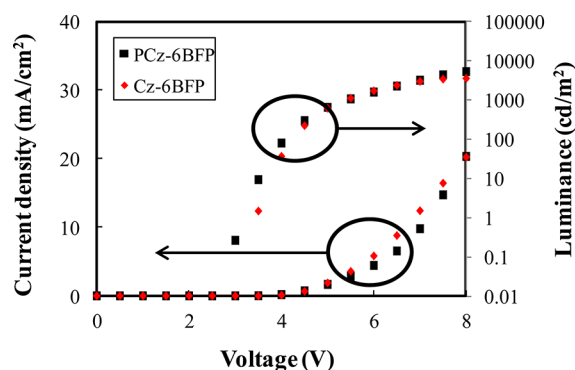


Figure 4. Current density–voltage–luminance curves of PCz-6BFP and Cz-6BFP blue PHOLEDs.

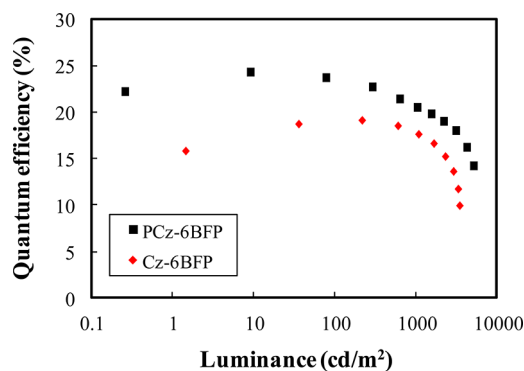


Figure 5. Quantum efficiency–luminance curves of PCz-6BFP and Cz-6BFP blue PHOLEDs.

emitting layer. It was reported that the electron current density of the emitting layer is reduced by doping the blue emitting FIrpic dopant in the emitting layer because of electron trapping by the FIrpic dopant.¹⁹ In the case of the Cz-6BFP device, the holes and electrons balance in the emitting layer is disrupted by the electron trapping effect of the FIrpic dopant in spite of similar hole and electron current density (Figure 3) without FIrpic doping. Therefore, the hole density in the emitting layer is higher than the electron density, resulting in relatively low quantum efficiency. On the contrary, the charge balance is improved in the PCz-6BFP device by the electron trapping effect. The electron current density of the PCz-6BFP device was higher than hole current density, but it is reduced by the electron trapping of FIrpic, which lead to better charge balance in the emitting layer. Therefore, high quantum efficiency was achieved in the PCz-6BFP device. The quantum efficiency of the PCz-6BFP device was better than that of PCz-BFP device. All device data of BFP derivatives are summarized in Table 2.

Table 2. Summarized Device Performances of BFP Derivatives

	quantum efficiency (%)	current efficiency (cd/A)	power efficiency (lm/W)	color coordinate
PCz-6BFP	24.3 ^a , 20.6 ^b	43.1 ^a , 36.3 ^b	43.3 ^a , 20.0 ^b	(0.14, 0.32)
Cz-6BFP	19.1 ^a , 17.7 ^b	32.7 ^a , 30.3 ^b	27.8 ^a , 19.1 ^b	(0.14, 0.31)

^a: Maximum efficiency. ^b: Efficiency at 1000 cd/m²

CONCLUSIONS

In conclusion, two host materials, PCz-6BFP and Cz-6BFP, were synthesized as high triplet energy bipolar host materials for blue PHOLEDs. 6- Position of the BFP core was easily substituted with carbazole or 9-phenylcarbazole using 6Cl-BFP intermediate prepared by ring closing reaction. The two host materials showed high triplet energy for efficient energy transfer to FIrpic dopant and gave high quantum efficiency in blue PHOLEDs. In particular, a high quantum efficiency of 24.3% was achieved using the PCz-6BFP host material. It can be concluded from this result that the modification of 6-position of the BFP core is effective to improve the quantum efficiency of blue PHOLEDs.

AUTHOR INFORMATION

Corresponding Author

*Fax: (+) 82-31-8005-3585. E-mail: lee17@dankook.ac.kr.

Notes

The authors declare no competing financial interest.

ACKNOWLEDGMENTS

This work was supported by LG display, GRRC program of Gyeonggi Province (GRRC Dankook2012-B01: Development of High Efficiency White OLED Materials and Their Devices), IT R&D program of MKE/KEIT [KI002104-2010-02], the Development of Core Technologies for Organic Materials Applicable to OLED Lighting with High Color Rendering Index by the Ministry of Knowledge and Economy (MKE) and the fundamental R&D Program for Core Technology of Materials (grant no. M2009010025) funded by the MKE.

REFERENCES

- (1) Tao, Y.; Yang, C.; Qin, J. *Chem. Soc. Rev.* **2011**, *40*, 2943–2970.
- (2) Chaskar, A.; Chen, H.-F.; Wong, K.-T. *Adv. Mater.* **2011**, *23*, 3876–3895.
- (3) Su, S.-J.; Sasabe, H.; Takeda, T.; Kido, J. *Chem. Mater.* **2008**, *20*, 1691–1701.
- (4) Chou, H.-H.; Cheng, C.-H. *Adv. Mater.* **2010**, *22*, 2468–2471.
- (5) Chopra, N.; Lee, J.; Zheng, Y.; Eom, S.-H.; Xue, J.; So, F. *Appl. Phys. Lett.* **2008**, *93*, 143307.
- (6) Jeon, S. O.; Jang, S. E.; Son, H. S.; Lee, J. Y. *Adv. Mater.* **2011**, *23*, 1436–1441.
- (7) Hsu, F.-M.; Chien, C.-H.; Shu, C.-F.; Lai, C.-H.; Hsieh, C.-C.; Wang, K.-W.; Chou, P.-T. *Adv. Funct. Mater.* **2009**, *19*, 2834–2843.
- (8) Liu, H.; Cheng, G.; Hu, D.; Shen, F.; Lv, Y.; Sun, G.; Yang, B.; Lu, P.; Ma, Y. *Adv. Funct. Mater.* **2012**, *22*, 2830–2836.
- (9) Hu, D.; Shen, F.; Liu, H.; Lu, P.; Lv, Y.; Liu, D.; Ma, Y. *Chem. Commun.* **2012**, *48*, 3015–3017.
- (10) Son, K. S.; Yahiro, M.; Imai, T.; Yoshizaki, H.; Adachi, C. *Chem. Mater.* **2008**, *20*, 4439–4446.
- (11) Rothmann, M. M.; Haneder, S.; Da Como, E.; Lennartz, C.; Schildknecht, C.; Strohhriegl, P. *Chem. Mater.* **2010**, *22*, 2403–2410.
- (12) Gong, S.; Chen, Y.; Yang, C.; Zhong, C.; Qin, J.; Ma, D. *Adv. Mater.* **2010**, *22*, 5370–5373.
- (13) Hua, D.; Cheng, G.; Liu, H.; Lv, Y.; Lu, P.; Ma, Y. *Org. Electron.* **2012**, *13*, 2825–2831.
- (14) Gong, S.; Chen, Y.; Luo, J.; Yang, C.; Zhong, C.; Qin, J.; Ma, D. *Adv. Funct. Mater.* **2011**, *21*, 1168–1178.
- (15) Lin, M.-S.; Yang, S.-J.; Chang, H.-W.; Huang, Y.-H.; Tsai, Y.-T.; Wu, C.-C.; Chou, S.-H.; Mondalb, E.; Wong, K.-T. *J. Mater. Chem.* **2012**, *22*, 16114–16120.
- (16) Ku, S.-Y.; Hung, W.-Y.; Chen, C.-W.; Yang, S.-W.; Mondal, E.; Chi, Y.; Wong, K.-T. *Chem. Asian J.* **2012**, *7*, 133–142.
- (17) Lee, C. W.; Lee, J. Y. *Adv. Mater.* **2013**, *25*, 596–600.
- (18) Su, S. J.; Cai, C.; Kido, J. *Chem. Mater.* **2011**, *23*, 274–284.
- (19) Cai, X.; Padmaperuma, A. B.; Sapochak, L. S.; Vecchi, P. A.; Burrows, P. E. *Appl. Phys. Lett.* **2008**, *92*, 083308.